

# The gravitational redshift of Sirius B

S. R. G. Joyce<sup>1</sup>, M. A. Barstow<sup>1</sup>, J. B. Holberg<sup>2</sup>, H. E. Bond<sup>3</sup>, S. L. Casewell<sup>1</sup>, M. R. Burleigh<sup>1</sup>

<sup>1</sup> Dept. of Physics & Astronomy, Leicester Institute of Space and Earth Observation, University of Leicester, University Road, Leicester, LE1 7RH ; srgj1@leicester.ac.uk, mab@le.ac.uk

<sup>2</sup> University of Arizona, LPL, Tucson, AZ 85721, USA ;

<sup>3</sup> Department of Astronomy & Astrophysics, Pennsylvania State University, University Park, PA 16802, USA

## Abstract

Previous measurements of the gravitational redshift of Sirius B have resulted in a mass estimate which is significantly larger than the mass measured from the binary orbit. We have obtained new *HST* observations of Sirius A and B in Cycle 25 which were used to make a differential measurement of the WD gravitational redshift. We measure a redshift of  $80.65 \pm 0.77 \text{ km s}^{-1}$  which, when combined with the radius, gives a mass of  $1.017 \pm 0.025 M_{\odot}$ . The new result is in agreement with the dynamical mass and the predictions of a C/O white dwarf mass-radius relation with a precision of 2.5 per cent.

## 1 Introduction

The strong gravitational field of a white dwarf causes light escaping from its surface to be redshifted by an amount proportional to the mass/radius ratio of the star (Einstein., 1916). This effect can be detected as a shift in the wavelength of the hydrogen absorption lines observed in the spectra of DA white dwarfs. If the radius is measured independently, the gravitational redshift provides a measurement of the mass. These mass and radius measurements can be compared to the predictions of the theoretical mass-radius relation (MRR) first developed by (Chandrasekhar, 1931). Detailed tests of the MRR require mass measurements with a precision of a few per cent in order to distinguish between models with different temperature and H-layer thickness. Such precision has been achieved for a small number of WDs in wide binaries using the dynamical method (e.g. Bond et al. 2017a,b) based on accurate orbit determinations. High precision ( $\sim 2.4\%$  uncertainty in mass) results have also been achieved for eclipsing binaries (Parsons et al., 2017), although no eclipsing systems have so far been found where the white dwarf mass is greater than  $0.84 M_{\odot}$ .

The gravitational redshift method has the potential to achieve a similar level of accuracy, but it has proven

difficult to correctly account for all of the systematics which can affect the measurements. One challenge with measuring the gravitational redshift is that the spectrum can also be shifted due to the space motion of the white dwarf. An independent measure of the radial velocity is required to determine how much each effect contributes to the observed wavelength shift. Sirius-Like Systems consisting of a white dwarf and a main sequence companion of type K or earlier (Holberg et al., 2013) are ideal because the radial velocity of the binary with respect to Earth can be measured from the main sequence star.

Sirius B itself is a prime target for testing the MRR because it has a precisely determined orbit and dynamical mass (Bond et al., 2017b) based on over 150 years of observations, including a long running campaign with *HST*. Observations of Sirius A have measured the radial velocity of the binary and the orbital motions so that these can be corrected for when making gravitational

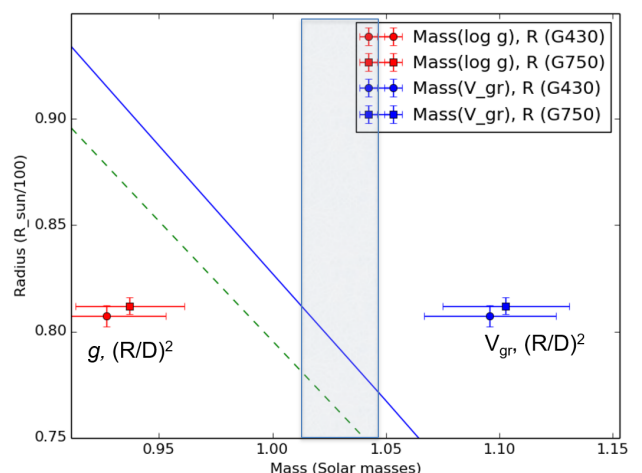


**Figure 1:** Analysis of *HST* spectra of Sirius B taken in 2013 confirmed that the mass from the gravitational redshift (blue) was significantly larger than the dynamical mass (shaded rectangle) and the predicted mass from the MRR (blue line). The mass derived using the spectroscopic method of Balmer line fitting (red) was also inconsistent with the other two methods. (Figure first presented in Barstow et al. 2017).

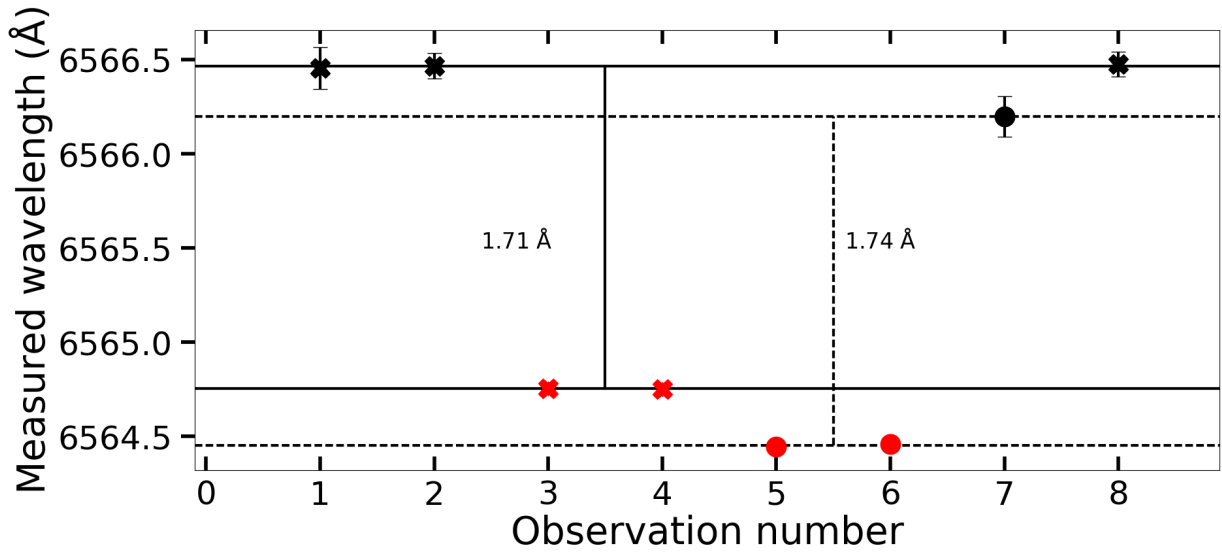


**Figure 2:** Measured wavelength for each spectrum in the order in which they were observed along the x axis. Colours indicate the target: Sirius A (red, lower markers) and Sirius B (black, upper markers). Shapes indicate the aperture used, E1 position (crosses) and “centre” (circles). Horizontal lines show the average wavelength and vertical lines indicate the difference in average wavelength between Sirius A and B.

redshift measurements of Sirius B.

The first modern CCD spectrum of Sirius B was obtained by Barstow et al. (2005) using the Space Telescope Imaging Spectrograph (STIS) on the Hubble Space Telescope (*HST*). The spectrum was of exceptional quality compared to ground based spectra, and free from contamination by light from Sirius A. Measurement of the shift in the  $H\alpha$  line compared to the rest wavelength measured in laboratories resulted in a gravitational redshift of  $80.42 \pm 4.83 \text{ km s}^{-1}$ . However, the mass calculated in that analysis could not be reconciled with the spectroscopic and dynamically measured masses to confirm consistency of the different techniques. A further set of STIS observations were carried out in 2013 (Barstow et al., 2017) and improved the precision further. Unfortunately, the data confirmed there was a definite discrepancy between the gravitational and dynamical mass of around 10 per cent which was larger than the measurement uncertainty as shown in Fig. 1.

The question remains as to whether this discrepancy was caused by a fundamental problem with the theory, or simply an instrumental effect. A resolution to this puzzle requires observations which can disentangle any potential systematic effect from the genuine gravitational redshift signal. We have obtained new *HST* observations of Sirius A and B which we are using to carry out a differential measurement of the shift in the wavelength of the  $H\alpha$  line (Joyce et al., 2018b). These observations have been performed by observing Sirius A and B with the same instrument setup over a single *HST* orbit so that it is possible to distinguish systematic instrumental effects from the gravitational redshift.

## 2 The observations

The data for this study were obtained as part of GO program 15237, (PI Joyce) in cycle 25 at the start of 2018. The data consist of 4 exposures each for Sirius A and B. All spectra were taken with the G750M grating which covers the wavelength range 6295 – 6867 Å and captures the broadened wings of the WD  $H\alpha$  line centred at  $\sim 6564 \text{ Å}$ . A slit was used to ensure that only light from the targeted star entered the spectrograph. The orientation of the spacecraft was selected so that the long slit would be perpendicular to the line joining Sirius A and B. This ensures that the slit does not go across both stars. The position of the target along the slit changes due to the use of both the standard position, with the spectrum at the centre of the CCD (row 512), and the pseudo E1 aperture position which places the spectrum closer to the top of the CCD (row 898).

The telescope was first pointed at Sirius B to obtain two exposures at the E1 position. The telescope was then moved to Sirius A and further exposures were taken without any intervening changes to the instrumental set up so as to minimise the possibility of systematics introduced by moving slits and filters. A total of four spectra were obtained for each target.

## 3 Analysis

All spectra of Sirius B were checked for possible contamination by light from Sirius A but no evidence of scattered light was found.

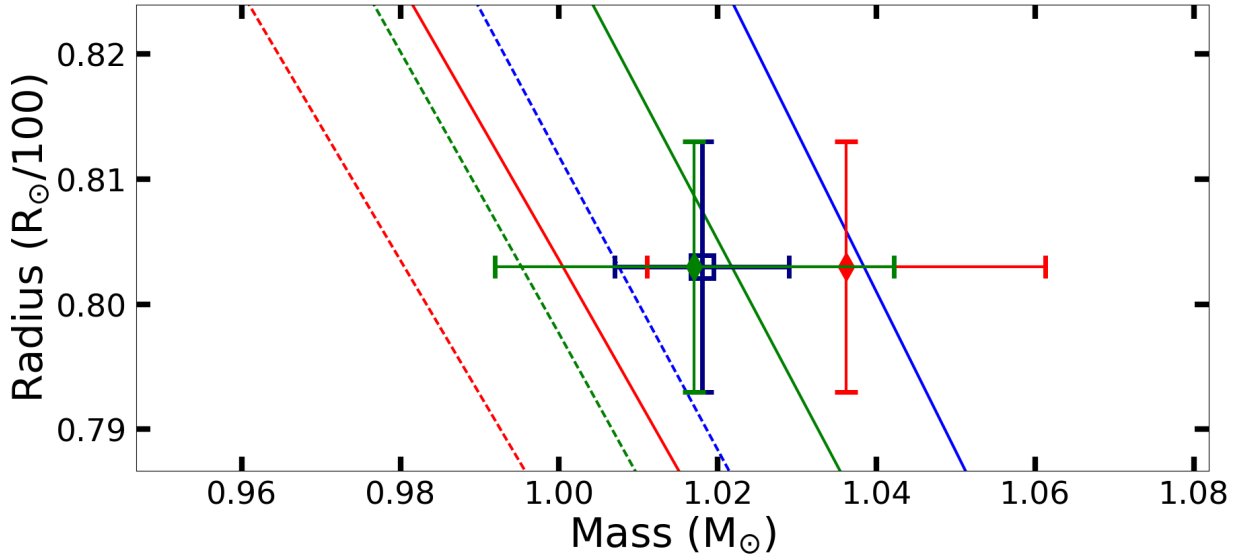


**Figure 3:** Mass measured from the gravitational red-shift at the E1 position (green diamond) compared to the mass from the dynamical method (dark blue square, Bond et al., 2017b). The red diamond (right) is the gravitational red-shift mass from the 'centre' position. The solid and dashed lines are Fontaine, Brassard & Bergeron (2001) C/O core mass-radius relations for thick and thin H-layer respectively. The (green) MRR is for a temperature of 25,922 K which is the appropriate  $T_{\text{eff}}$  for Sirius B according to the spectroscopic fits to the G430 data. Red and blue lines either side are for 10,000 K and 40,000 K respectively.

The wavelength of the observed  $H\alpha$  line in the Sirius A and B spectra was measured by fitting a Lorentzian model to the core of the line. The fitting makes no assumption about the rest wavelength and is simply a measure of the wavelength at the centre of the line.

To accurately measure the wavelength of the line centre, the fitting for each line was repeated four times with a slightly increased wavelength range each time. The ranges used are 7, 11, 15 and 19 Å. These were chosen so as to focus on the sharply defined line core and avoid including too much of the wings which may be affected by the Stark pressure shift and asymmetry. Tests of lab based plasma have shown that the Stark shift in the  $H\alpha$  line increases with increasing distance from the line core (Halenka et al., 2015). For the wavelength ranges we have chosen (7 – 19 Å), the effect of the Stark shift is expected to be below  $1 \text{ km s}^{-1}$  based on simulations and observations of plasma in the laboratory (Halenka et al. 2015, see their Fig. 13).

The observed velocity is calculated from the difference in the measured wavelengths between Sirius A and Sirius B. Fig. 2 shows the measured wavelength of each  $H\alpha$  line in the order in which they were observed. The markers are black for Sirius B and red for Sirius A. This clearly highlights the difference caused by using the E1 position (diamonds) compared to the centre position (circles). The horizontal lines indicate the average wavelength measured for the E1 spectra (solid line) and centre spectra (dashed line). The wavelength difference is converted into a velocity using

equation (1):

$$v_{\text{obs}} = \frac{\lambda_B - \lambda_A}{\lambda_A} \times c. \quad (1)$$

The observed velocity was corrected by adding  $3.198 \text{ km s}^{-1}$  to account for the relative motion between Sirius A and B resulting from the binary orbital motion. Corrections were also applied for the motion of *HST* as the telescopes orbital motion moves it towards or away from the target at up to  $\pm 7.5 \text{ km s}^{-1}$ . There is also a correction of  $-0.759 \text{ km s}^{-1}$  for the gravitational redshift of Sirius A.

## 4 Results

For the spectra taken at the E1 position, the final velocity attributed to the gravitational redshift ( $v_{\text{gr}}$ ) is  $80.65 \pm 0.77 \text{ km s}^{-1}$ . The mass is calculated from  $v_{\text{gr}}$  and the radius using equation (2). In this equation  $v_{\text{gr}}$  is in  $\text{km s}^{-1}$  and  $M$  and  $R$  are in solar units. The radius of  $0.803 \pm 0.011 R_{\odot}/100$  was calculated from the flux in the G430L spectra as described in Joyce et al. (2018a) and uses a parallax of  $378.9 \pm 1.4$  milliarcseconds from Bond et al. (2017b):

$$M = \frac{v_{\text{gr}} R}{0.636}. \quad (2)$$

The E1 spectra give a mass of  $1.017 \pm 0.025 M_{\odot}$ . For the spectra taken at the centre of the CCD, the same process gives a slightly larger mass of  $1.036 \pm 0.025 M_{\odot}$ . The mass resulting from the differential

redshift measurement is in excellent agreement with the theoretical MRR for a C/O core WD with a  $T_{\text{eff}}$  of 25,922 K (Fontaine, Brassard & Bergeron, 2001) shown by the green line in Fig. 3. This is clear evidence that white dwarfs follow the expected trend of decreasing radius with increasing mass.

For comparison, the dynamical mass from Bond et al. (2017b) is also plotted (blue square). The data points for the E1 redshift (green diamond) and dynamical mass (blue square) are directly on top of one another despite being obtained using completely different methods.

## 5 Conclusions

Our analysis has shown that the gravitational redshift method is a reliable and accurate way of measuring the mass of a white dwarf. However, there are a number of corrections and systematic effects which must be carefully considered before attributing the measured wavelength shift to the gravity of the white dwarf. Any movement of the source or detector produces a Doppler shift in the spectrum which is indistinguishable from the gravitational shift unless further information is available. Furthermore, the calibration of the spectrum, and the rest wavelength it is compared to, can systematically alter results. The differential method, where a companion star spectrum is used as a reference, can successfully reveal these sources of error.

## Acknowledgements

Special thanks to Blair Porterfield, Joleen Carlberg and the team at STScI for all their help and advice during the phase 2 proposal. SRGJ acknowledges support from the Science and Technology Facilities Council (STFC, UK). MAB acknowledges support from the Gaia post-launch support programme of the UK Space Agency and the Leicester Institute for Space and Earth Observation (LISEO). SLC acknowledges support from LISEO. JBH and HEB acknowledge support provided by NASA through grants from the Space Telescope Science Institute, which is operated by the Association of Universities for Research in Astronomy, Inc., under NASA contract NAS5-26555.

## References

- Barstow, M. A., Bond, H. E., Holberg, J. B., et al. 2005, *MNRAS*, 362, 1134
- Barstow, M. A., Joyce, S., Casewell, S. L., et al. 2017, 20th European White Dwarf Workshop, 509, 383
- Bond, H. E., Bergeron, P., & Bédard, A. 2017a, *ApJ*, 848, 16
- Bond, H. E., Schaefer, G. H., Gilliland, R. L., et al. 2017b, *ApJ*, 840, 70
- Chandrasekhar, S. 1931, *MNRAS*, 91, 456, "The Highly Collapsed Configurations of a Stellar Mass"
- Einstein, A., 1916, "The foundation of the general theory of relativity", *Annalen der Physik* 354, 769-822
- Fontaine, G., Brassard, P., & Bergeron, P. 2001, *PASP*, 113, 409
- Halenka, J., Olchawa, W., Madej, J., & Grabowski, B. 2015, *ApJ*, 808, 131
- Holberg, J. B., Oswalt, T. D., Sion, E. M., Barstow, M. A., & Burleigh, M. R. 2013, *MNRAS*, 435, 2077
- Joyce, S. R. G., Barstow, M. A., Casewell, S. L., et al. 2018a, *MNRAS*, 479, 1612
- Joyce, S. R. G., Barstow, M. A., Holberg, J. B., et al. 2018b, *MNRAS*, 481, 2361
- Parsons, S. G., Gänsicke, B. T., Marsh, T. R., et al. 2017, *MNRAS*, 470, 4473